14-line multiplet at 3.05 ppm for the SCH_2CH_2S protons. The low-temperature spectrum (235 K) shows considerable broadening, but no limiting spectrum could be attained. Since the solid-state conformation of the complex contains five different sets of methylene groups, some type of fluxional process must be occurring. A process in which the nonbonded S atoms, S2 and S5, interconvert with coordinated S atoms, S1 and S6, is most likely. This process would interconvert the five- and seven-membered chelate rings and should be relatively facile, since the conformation of the coordinated 16S6 macrocycle already orients the nonbonded S atoms toward the metal center.

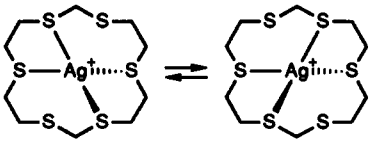

The possibility of oxidation of the Ag(I) cation to a stable Ag(II) species, which has been observed for $[Ag(9S3)_2]^+$ and $[Ag(18S6)]^+$, was investigated.[2-4] Cyclic voltammetry of $[Ag(16S6)]^+$ in CH_3CN (0.1 M $[NBu_4][PF_6]$) at platinum electrodes showed an oxidation at E_{pa} = 0.87 V versus Fc/Fc^+, which is essentially irreversible; only a small return wave was observed, indicating that the oxidized product is unstable in CH_3CN at 298 K. Attempts to stabilize the oxidation product in strongly aqueous media by the addition of H_2SO_4 (98%) or $HClO_4$ (70%) to $[Ag(16S6)]^+$, at 298 K, resulted in the production of a blue solution visible at the surface of the crystals as they dissolved. The color faded very quickly, and the crystals ultimately dissolved to give a clear solution. Although these observations are consistent with the generation of $[Ag(16S6)]^{2+}$, the transient nature of the product prevented a full analysis.

Discussion

The solid-state structure of $[Ag(16S6)]^+$ shows that the 16S6 macrocycle provides a unique coordination environment for Ag(I). This complex is four-coordinate, with two additional S donor atoms oriented toward the Ag^+ ion at distances approximately 0.8 Å longer than the coordinated Ag-S bond lengths. The solution ^1H NMR data for $[Ag(16S6)]^+$ also indicate that the two additional S atoms can participate in bonding to the metal center via an interconversion of bonded and nonbonded pairs of S donor atoms in the SCH_2S fragments. Therefore, the possibility exists that 16S6 could provide a distorted version of the S_6 coordination sphere found in $[Ag(18S6)]^+$ and necessary to stabilize Ag(II).[2]

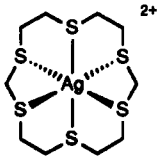

Electrochemically the oxidation chemistry of $[Ag(16S6)]^+$ appears to be similar to that observed for $[Ag(18S6)]^+$ and $[Ag(9S3)_2]^+$.[2-4] The homoleptic thioether coordination spheres found in $[Ag(18S6)]^+$, $[Ag(9S3)_2]^+$, and $[Ag(16S6)]^+$ result in relatively low oxidation potentials, E_{pa} = 1.00, 0.79, and 0.87 V, respectively. This can be attributed to a higher electron density at the metal center, which promotes oxidation. Stabilization of the deep blue oxidation products $[Ag(18S6)]^{2+}$ and $[Ag(9S3)_2]^{2+}$ is a direct result of the pseudooctahedral coordination geometries, which stabilizes Ag(II) with little structural rearrangement.[2] Structural and spectroscopic data suggest six sulfur atoms are involved in coordination to Ag(I) in $[Ag(16S6)]^+$, but the degree to which 16S6 can stabilize the Ag(II) oxidation product is limited. These results demonstrate the unique nature of 16S6 coordination and emphasize the structural requirements of the Ag(I)/Ag(II) redox couple.

Acknowledgment. We thank the Natural Sciences and Engineering Research Council of Canada and the donors of the Petroleum Research Fund, administered by the American Chemical Society, for financial support of this research.

Supplementary Material Available: Listings of crystallographic data collection parameters, positional parameters, thermal parameters, nonessential bond distances and angles, and hydrogen atom parameters (Tables S-I-S-V) (3 pages); listing of observed and calculated structure factors (Table S-VI) (12 pages). Ordering information is given on any current masthead page.

Contribution from the Laboratoire de Chimie Moléculaire, UA CNRS 426, Université de Nice, Parc Valrose, 06034 Nice, France, and Laboratoire de Cristallochimie, CNRS UA 254, Campus de Beaulieu, Université de Rennes, 35042 Rennes, France

Preparation and Structure of a Mixed Niobium(I) Isocyanide Carbonyl Complex with a Bent C-N-C Linkage

Ghazar Aharonian,[1a] Liliane G. Hubert-Pfalzgraf,*[,1a] Abdenasser Zaki,[1a] and Guy Le Borgne[1b]

Received November 27, 1990

Introduction

Inorganic and organometallic complexes in low oxidation states generally require good π-acceptor ligands. While carbon monoxide is a π-acceptor commonly used for this purpose, the isoelectronic isocyanide ligand may also stabilize low-valent species, although it has received less attention. Thus, while niobium carbonyl derivatives range from oxidation states +3 to -3, isocyanide complexes are limited to some trivalent species, $(\eta^5\text{-Cp})_2Nb(C_4H_9)(CNR)$ (R = Ph, Cy),[2] $[(\eta^5\text{-Cp})Nb(CN\text{-}t\text{-Bu})_4Cl]^+$,[3] $Nb_2Cl_6(CN\text{-}t\text{-Bu})_4(\mu\text{-}t\text{-BuNCCN-}t\text{-Bu})$,[4] and $Nb_3Cl_8(CN\text{-}t\text{-Bu})_5$.[5] No niobium or tantalum isocyanide complexes in oxidation states lower than 2 have been mentioned. We wish now to report the synthesis of the formally niobium(I) $NbCl(CO)(t\text{-BuNC})(dmpe)_2$ (dmpe = 1,2-dimethylphosphinoethane) derivative and its structural characterization, which shows the presence of a terminal bent carbene-like isocyanide moiety.

Experimental Section

All manipulations were routinely performed by using Schlenk tubes and vacuum-line techniques under purified argon. The solvents were purified by standard methods. $NbCl_5$ and dmpe were used as received; tBuNC was dried over molecular sieves. $NbCl(CO)_2(dmpe)_2$ was prepared according to the literature.[6] ^1H NMR and IR spectra were run on Bruker WH-90 and IR-FT S45 spectrometers, respectively. Elemental analysis was performed by the Centre de Microanalyse du CNRS.

$NbCl(CO)(t\text{-BuNC})(dmpe)_2$. *tert*-Butyl isocyanide (0.39 mL, 3.43 mmol) was added to a suspension of $NbCl(CO)_2(dmpe)_2$ (0.92g, 1.71 mmol) in 20 mL toluene at room temperature. The reaction medium was irradiated for 25 h (125 W). Filtration left a beige precipitate (analyzing as $Nb_2Cl_2(CN\text{-}t\text{-Bu})_3(dmpe)$) and a red-brown filtrate, which was concentrated and stored at -30 °C. Red crystals of $NbCl(CO)(t\text{-BuNC})(dmpe)_2$ (0.4g, 43%), suitable for X-ray, were obtained by precipitation and isolated by filtration. The product is insoluble in toluene and soluble in chloroform or methylene chloride. ^1H NMR (CD_2Cl_2, ppm): 1.42, (Me-P, m, 24 H), 0.98 (P-CH_2, m, 8 H), 1.24 (*t*-BuNC, s, 9 H). IR (Nujol, cm^{-1}): 1871, 1850 (ν(C—O)), 1747 (ν(N═C)), 300

(1) (a) Université de Nice. (b) Université de Rennes.
(2) Klazinga, A. H.; Teuben, J. H. *J. Organomet. Chem.* **1980**, *194*, 309.
(3) Aspinall, H. C.; Roberts, M. M.; Lippard, S. J. *Inorg. Chem.* **1984**, *23*, 1782.
(4) Cotton, F. A.; Duraj, S. A.; Roth, W. J. *J. Am. Chem. Soc.* **1984**, *106*, 6987.
(5) Cotton, F. A.; Roth, W. J. (a) *J. Am. Chem. Soc.* **1983**, *105*, 3734; (b) *Inorg. Chim. Acta* **1987**, *126*, 161.
(6) Burt, R. J.; Leigh, G. J.; Hughes, D. L. *J. Chem. Soc., Dalton Trans.* **1981**, 793.

0020-1669/91/1330-3105$02.50/0

Table I. Crystallographic Data for $Nb(CO)Cl(t\text{-BuNC})(dmpe)_2$

chem formula	$Nb(CO)Cl(t\text{-BuNC})(dmpe)_2$
a, Å	16.600 (7)
b, Å	11.012 (8)
c, Å	14.650 (7)
α, deg	90
β, deg	89.98 (6)
γ, deg	90
V, Å^3	2678.0
Z	4
fw	$NbClP_4ONC_{18}H_{41}$
space group	monoclinic, $P2_1/n$ (No. 14)
T, °C	−113
λ, Å	0.71073
ρ_{calcd}, g·cm^{-3}	1.437
μ, cm^{-1}	7.7
transm coeff	0.88–1.11
R	0.047
R_w	0.059

Table II. Positional Parameters for $NbCl(CO)(t\text{-BuNC})(dmpe)_2$ (Standard Deviations in Parentheses)

atom	x	y	z	B,[a] Å^2
Nb	0.24597 (4)	0.22211 (8)	0.01821 (5)	1.24 (1)
Cl	0.1485 (1)	0.1941 (2)	−0.1214 (1)	2.68 (5)
P1	0.2509 (1)	−0.0140 (2)	0.0184 (2)	1.47 (4)
P2	0.1177 (1)	0.1522 (2)	0.1002 (2)	1.91 (5)
P3	0.3542 (1)	0.2755 (3)	−0.1044 (2)	2.49 (5)
P4	0.2221 (2)	0.4444 (3)	−0.0230 (2)	2.68 (5)
O1	0.2565 (4)	0.3533 (6)	0.2106 (4)	3.3 (2)
N1	0.4143 (4)	0.1629 (7)	0.1208 (5)	2.1 (2)
C1	0.2527 (5)	0.3045 (9)	0.1401 (6)	2.2 (2)
C2	0.3519 (5)	0.1858 (7)	0.0852 (6)	1.6 (2)
C3	0.4684 (5)	0.197 (1)	0.1954 (6)	2.8 (2)
C4	0.4737 (7)	0.334 (1)	0.1993 (7)	3.9 (2)
C5	0.4311 (8)	0.154 (1)	0.2844 (7)	4.9 (3)
C6	0.5503 (6)	0.139 (1)	0.1757 (8)	7.2 (3)
C7	0.1644 (5)	−0.0862 (9)	0.0782 (6)	2.2 (2)
C8	0.3364 (5)	−0.0979 (9)	0.0684 (6)	2.3 (2)
C9	0.2424 (5)	−0.0838 (9)	−0.0957 (5)	2.3 (2)
C10	0.0906 (5)	−0.0032 (9)	0.0669 (6)	2.2 (2)
C11	0.0213 (5)	0.232 (1)	0.0788 (8)	3.7 (2)
C12	0.1181 (6)	0.143 (1)	0.2257 (6)	3.3 (2)
C13	0.4621 (6)	0.247 (1)	−0.0854 (7)	5.5 (3)
C14	0.3408 (6)	0.201 (1)	−0.2154 (6)	3.6 (3)
C15	0.3548 (7)	0.436 (1)	−0.1372 (7)	4.5 (3)
C16	0.2624 (8)	0.564 (1)	0.0513 (8)	5.3 (3)
C17	0.1181 (6)	0.502 (1)	−0.0415 (8)	4.2 (3)
C18	0.2695 (7)	0.485 (1)	−0.1366 (7)	4.0 (3)

[a] Values for anisotropically refined atoms are given in the form of the isotropic equivalent displacement parameter defined as $(4/3)[a^2B(1,1) + b^2B(2,2) + c^2B(3,3) + ab(\cos\gamma)B(1,2) + ac(\cos\beta)B(1,3) + bc(\cos\alpha)b(2,3)]$.

(ν(Nb—Cl)). Mass spectrum (Cl, NH_3), M = $NbCl(CO)(t\text{-BuNC})(dmpe)_2$: M (73%), M − CO (12%), M − HCl (100%), $dmpeH_2$ (69%).

X-ray Crystallographic Procedure. Crystal and data collection information is summarized in Table I. Intensity data were collected on an Enraf-Nonius CAD-4 automatic diffractometer, at T = −113 °C. Lorentz and polarization effects were corrected, and an empirical absorption correction using the program DIFABS was applied. Cell parameters were refined by using the angles of 25 reflections measured on the diffractometer.

The structure was solved on a PDP 11/60 computer with the SDP package. Atomic positions of the 26 non-hydrogen independent atoms were found with the program MULTAN and subsequent Fourier-difference synthesis. Refinement of coordinates and thermal parameters, first isotropic and then anisotropic, of these 26 atoms led to final values of R = 0.047 and R_w = 0.059, using 2457 reflections with $I > 2\sigma(I)$. No attempt was made to introduce hydrogen atoms. Positional parameters are listed in Table II.

Results

The photochemical reaction of 2 equiv of *tert*-butyl isocyanide with $NbCl(CO)_2(dmpe)_2$ produced the carbonyl–isocyanide complex $NbCl(CO)(t\text{-BuNC})(dmpe)_2$ (**1**) in 40% yield together with a isocyanide complex analyzing as $[Nb_2Cl_2(t\text{-BuNC})_3(dmpe)]_n$ (**2**) (18%) and unreacted starting material. The formation of the latter product is favored by an increase of the amount of the isocyanide ligand since more than 1 equiv of this ligand is required in order to obtain **1** in a good yield. Although **2** is difficult to characterize in view of its insolubility, the presence in the IR region of a NH absorption at 3315 cm^{-1} suggests a C=NH(*t*-Bu) ligand in the coordination sphere,[7] together with terminal isocyanide ligands (ν(NC) = 2093, 1977 cm^{-1}).

$NbCl(CO)(t\text{-BuNC})(dmpe)_2$ appears through mass spectrometry to be monomeric. Its IR spectrum mainly shows the carbonyl absorptions (1871, 1850 cm^{-1}) and a broad band corresponding to the C=N stretches at an unusual low energy, 1747 cm^{-1}. A structure study, whose results are presented in Tables I and II, was thus undertaken.

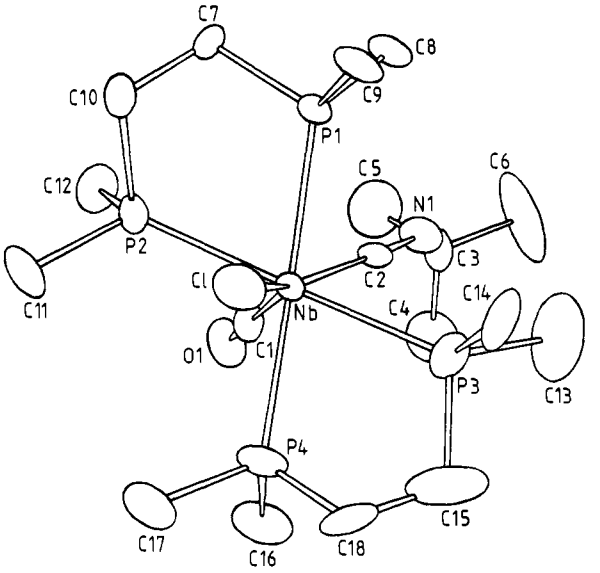

Figure 1. Structure of $NbCl(t\text{-BuNC})(CO)(dmpe)_2$, indicating the atomic numbering scheme. Thermal ellipsoids are at 50% probability.

Table III. Selected Interatomic Distances (Å) and Angles (deg) for $NbCl(CO)(t\text{-BuNC})(dmpe)_2$ (Standard Deviations in Parentheses)

	Coordination Sphere		
Nb–Cl	2.627 (2)	Nb–P4	2.552 (2)
Nb–P1	2.595 (2)	Nb–C1	2.007 (7)
Nb–P2	2.563 (2)	Nb–C2	2.054 (7)
Nb–P3	2.607 (2)		
Cl–Nb–P1	84.45 (6)	P2–Nb–P3	164.36 (6)
Cl–Nb–P2	79.51 (6)	P2–Nb–P4	105.64 (7)
Cl–Nb–P3	85.10 (6)	P2–Nb–C1	76.4 (2)
Cl–Nb–P4	80.36 (7)	P2–Nb–C2	115.4 (2)
Cl–Nb–C1	141.3 (2)	P3–Nb–P4	74.22 (8)
Cl–Nb–C2	151.3 (2)	P3–Nb–C1	118.2 (2)
P1–Nb–P2	74.08 (7)	P3–Nb–C2	77.5 (2)
P2–Nb–P3	101.79 (7)	P4–Nb–C1	77.6 (2)
P1–Nb–P4	164.56 (7)	P4–Nb–C2	115.6 (2)
P1–Nb–C1	116.7 (2)	C1–Nb–C2	67.3 (3)
	Ligands		
O1–C1	1.166 (8)		
N1–C2	1.186 (8)	N1–C3	1.464 (8)
C3–C4	1.52 (1)	C7–C10	1.537 (9)
C3–C5	1.52 (1)	C15–C18	1.52 (1)
C3–C6	1.52 (1)		
C2–N1–C3	144.1 (7)	Nb–C2–N1	177.4 (6)
Nb–C1–O1	179.4 (7)		

Discussion

The crystal structure of $NbCl(CO)(t\text{-BuNC})(dmpe)_2$ consists of discrete heptacoordinated molecules (Figure 1), and shows the

(7) Barder, T. J.; Powell, D.; Walton, R. A. *J. Chem. Soc., Chem. Commun.* **1985**, 550.

Table IV. Structural Data for Terminal Isocyanide Ligands in Various Complexes

complex	Nb-C, Å	C-N, Å	C-N-C, deg	ref
$NbCl(CO)(t\text{-BuNC})(dmpe)_2$	2.054 (7)	1.186 (8)	1.441 (7)	*a*
$[(\eta^5\text{-Cp})NbCl(t\text{-BuNC})_4]^+$	2.203 (9)-2.210 (10)	1.133 (12)-1.139 (13)	171.0 (10)-174.3 (10)	3
$Nb_2Cl_6(t\text{-BuNC})_6$	2.226 (13)-2.299 (14)	1.12 (2)-1.151 (15)	169 (1)-178 (2)	4
$Nb_3Cl_8(t\text{-BuNC})_5$	2.202 (12)-2.266 (13)	1.116 (13)-1.173 (14)	173 (1)-178 (1)	5

[a] This work.

bending of the RNC ligand. Relevant interatomic distances and angles are collected in Table III. No short contacts are observed.

The structure is best described as a monocapped-trigonal-prismatic coordination polyhedron with the chlorine in the capping position, the phosphorus atoms in the capped quadrilateral face, and the π-acceptor carbonyl and isocyanide ligands on the remaining edge. It shows similarities with the geometry of $Nb(OArMe_2\text{-}3,5)(CO)_2(dmpe)_2$[8] and that of $TaCl(CO)_3(PMe_3)_3$.[9]

The salient features of the structure appear in the form of a severe bending in the C-N-C linkage, a fairly short Nb-C bond length, and a long Nb-Cl bond length. Table IV lists the data for the structurally characterized niobium isocyanide complexes. The reduced Nb-C-N bond angle (144.1 (7)°) as well as the short Nb-C bond length (2.054 (7) Å) accounts for a carbene-like isocyanide moiety:[10,11]

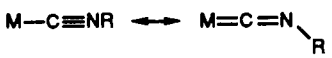

This Nb-C distance is much shorter than the values usually found for single order niobium-carbon bonds (~2.32 Å) and is in agreement with the distances observed for niobium metallocyclopropenes[12] or in tantalum alkylidenes[13] (1.93-2.07 Å). Back-bonding into one π^* bonding orbital of *t*-BuNC is favored by the low oxidation state of the metal as well as by the presence of the dmpe ligands in the coordination sphere. This bent tBuNC ligand thus accounts for the low ν(NC) frequency in the IR, as opposed to the typical values found for niobium complexes having almost linear isocyanide ligands (2185-2048 cm^{-1}, for instance, for $[(\eta^5\text{-Cp})Nb(t\text{-BuNC})_4Cl]^+$[3]). Bent terminal isocyanide ligands have also been proposed for the $(\eta^5\text{-Cp})_2MR'(RNC)$ complexes (M = Nb, Ta),[14] although no structural characterization was achieved.

The Nb-Cl bond distance of 2.627 (2) Å is unusually long and is even significantly longer than the greatest value reported for a terminal Nb-Cl bond (2.505 (4) Å).[3] Comparison of the Nb-Cl bond lengths in various derivatives reveals a progressive lengthening as the metal oxidation state decreases from 5 to 4 and to 3.[3] $NbCl(CO)(t\text{-BuNC})(dmpe)_2$ is to our knowledge the first structurally characterized mononuclear niobium(I) chlorine derivative reported so far.

The geometry observed for the diphosphine is similar to that frequently found for this ligand:[13,15,16] Pb-Nb-P bite angles of 74.08 (7) and 74.22 (8)° with Nb-P bond lengths ranging from 2.552 (2) to 2.607 (2) Å.

Acknowledgment. We are grateful to Dr. R. Astier for X-ray data collection and to Professor D. Grandjean for the use of the PDP/60 computer.

Supplementary Material Available: Tables of crystal data, intermolecular distances and angles, and anisotropic temperature parameters (3 pages); a listing of observed and calculated structure factor amplitudes (14 pages). Ordering information is given on any current masthead page.

(8) Coffindaffer, T. W.; Rothwell, I. P.; Folting, K.; Huffman, J. C.; Sterb, W. E. *J. Chem. Soc., Chem. Commun.* **1985**, 1519.
(9) Luetkens, M. L.; Santure, D. J.; Huffman, J. C.; Sattelberger, A. P. *J. Chem. Soc., Chem. Commun.* **1985**, 552.
(10) Yamamoto, Y. *Coord. Chem. Rev.* **1980**, *32*, 193.
(11) Singleton, E.; Oosthuizen, H. E. *Adv. Organomet. Chem.* **1983**, *22*, 209.
(12) Hey, E.; Weller, F.; Dehnicke, K. *Z. Anorg. Allg. Chem.* **1984**, *514*, 25.
(13) Holloway, C. E.; Melnik, M. *J. Organomet. Chem.* (a) **1986**, *303*, 1. (b) Idem *J. Organomet. Chem.* **1986**, *303*, 39.
(14) Klazinga, A. H.; Teuben, J. H. *J. Organomet. Chem.* **1980**, *192*, 75.
(15) Meakin, P.; Guggenberger, L. J.; Tebbe, F. N.; Jesson, J. P. *Inorg. Chem.* **1974**, *13*, 1025.
(16) Albright, J. O.; Datta, S.; Dezube, B.; Kouba, J. K.; Marynick, D. S.; Wreford, S. S.; Foxman, B. M. *J. Am. Chem. Soc.* **1979**, *101*, 611. Bianconi, P. A.; Williams, I. D.; Engeler, M. P.; Lippard, S. J. *J. Am. Chem. Soc.* **1986**, *108*, 311.

Contribution from the Institut für Organische Chemie, Universität Erlangen-Nürnberg, Henkestrasse 42, D-8520 Erlangen, Germany, Institute of Organic Chemistry and Biochemistry, Czechoslovak Academy of Sciences, 16618 Prague 6, CSFR, and Institute of Inorganic Chemistry, Czechoslovak Academy of Sciences, 25068 Řež near Prague, CSFR

On the Origin of the Antipodal Effect in *closo*-Heteroboranes

M. Bühl,[†] P. v. R. Schleyer,*[,†] Z. Havlas,[‡] D. Hnyk,[§] and S. Heřmánek[§]

Received November 27, 1990

Introduction

One of the main factors governing the ^{11}B chemical shifts in heteroboranes is the "antipodal" effect or A-effect.[1,2] The replacement of a boron nucleus in a polyhedral borane by a heteroatom (or group) X results in a downfield $\delta(^{11}B)$ chemical shift for the boron across the cage from X. Even though farthest away, the antipodal boron often undergoes the largest chemical shift change of all nuclei that are influenced by X.

The origin of the A-effect has been the topic of several empirical[1,2] and theoretical[3,4] investigations. Heřmánek, Hnyk, and Havlas (HHH) noticed a linear correlation of $\delta(^{11}B)$ of the antipodal atom in 10- and 12-vertex cages with *p* densities (charges) obtained from CNDO/2 calculations.[3] Fehlner, Czech, and Fenske (FCF) compared the paramagnetic chemical shift components in $B_{10}H_{10}^{2-}$ and B_9H_9NH employing the Fenske-Hall MO method.[4] They ascribed the enhanced paramagnetic (deshielding) contributions in the aza compound to a smaller energetic difference ΔE between suitable occupied and unoccupied MO's and to a larger "antipodal B-" character of these MO's with respect to the boron homologue.

We have been using the IGLO (individual gauge for localized orbitals) method[5] to calculate ^{11}B chemical shifts for boron compounds.[6] Remarkable precision can be achieved provided accurate geometries are employed.

Our objective was to test if IGLO calculations at a modest level of theory could reproduce the large chemical shift differences associated with the antipodal effect. In addition, we expected further information concerning the origin of this effect. The largest

[†] Universität Erlangen-Nürnberg.
[‡] Institute of Organic Chemistry and Biochemistry, Czechoslovak Academy of Sciences.
[§] Institue of Inorganic Chemistry, Czechoslovak Academy of Sciences.

0020-1669/91/1330-3107$02.50/0